RSC Advances

PAPER

View Article Online
View Journal | View Issue

Cite this: *RSC Adv.*, 2022, **12**, 17217

Phase change composites of octadecane and gallium with expanded graphite as a carrier

Yuchen Yao, [ab] Yuntao Cui [a] and Zhongshan Deng*[ab]

Received 29th April 2022
Accepted 28th May 2022

DOI: 10.1039/d2ra02734h

rsc.li/rsc-advances

Phase change materials (PCMs) have attracted more and more attention in the field of energy and thermal management due to the characteristic of exchanging heat with small temperature change. In order to obtain perfect PCMs, previous researchers usually prepared various phase change composites (PCCs), but there is still a gap toward the goal. Perhaps the development of PCMs with adjustable properties in a wide range to meet different needs is a feasible option. Given that the properties of organic PCMs and metal PCMs are highly complementary, using expanded graphite (EG) as a mediator, a stable PCC of octadecane and gallium that are difficult to directly mix, was successfully prepared. Octadecane and gallium are stored in the microstructures of EG, and the microstructures of EG play the role of storing nucleation embryos, and the suppression of supercooling can reach more than 86.82%. The test results showed that the properties of the PCC are indeed a balance between octadecane and gallium, and can be adjusted in a wide range. The PCC also has good structural and chemical stability, which can effectively avoid the corrosion risk caused by gallium leakage. The PCC samples containing equal amounts of gallium and paraffin were selected for thermal management performance tests. The results indicated that the PCC has application potential in related fields, and can provide a reference for the development of other PCCs.

1. Introduction

Phase change materials (PCMs) have received great attention in the fields of energy storage and thermal management, for the fact that they can absorb or release a large amount of heat without a significant change in temperature. According to the species of matter, PCMs can be divided into two main categories: the organic and the inorganic. The organic PCMs are represented by paraffins, fatty acids, esters and polymers, which have the characteristics of high latent heat per unit mass, low thermal conductivity, and large volume change between solid and liquid states, while the inorganic PCMs mainly include molten salts, hydrated salts and metal.[1,2] Metal PCMs have attracted much attention in recent years, due to their outstanding advantages in high thermal conductivity, high latent heat per unit volume and small volume change before and after phase change.[2,3] In particular, the value of low melting point metal or so called "liquid metal" represented by gallium in passive thermal management has long been reported,[4,5] and some recent studies also demonstrated its potential in thermoregulation and aerospace.[6,7] The advantages and disadvantages of the above PCMs are very clear.

In order to obtain the best possible PCM, it is usually necessary to prepare phase change composite (PCC) composed of pure PCMs and functional materials to maximize strengths and avoid weaknesses. With the purpose to overcome the disadvantage in thermal conductivity, organic PCMs are often mixed with thermal conductivity enhancers or packed into thermally conductive matrix.[8] For example, Raj *et al.* achieved over 60% thermal conductivity increase by adding multi-wall carbon nano tubes/graphene nano platelets to an organic form-stable PCM.[9] Expanded graphite (EG) is a kind of classic matrix with high thermal conductivity. In the study of Zhang *et al.*, while improving the thermal conductivity of PCMs, EG with excellent absorbability can also prevent the leakage of melted paraffin under the action of capillary force and surface tension.[10] By compounding with EG, Wang *et al.* improved the thermal conductivity of the sebacic acid (SA) PCC and suppressed the supercooling.[11] Wu *et al.* also impregnated SA into the EG matrix and obtained a PCC with anisotropic thermal conductivity after being compressed into a block, and the thermal conductivity was approximately 130 times higher than that of pure PCMs.[12] In addition to EG, metal foam is another kind of commonly used matrix. Numerical studies by Duan pointed out that PCMs combined with metal foam can enhance the cooling effect for concentrating photovoltaics.[13] Since the basic thermal conductivities of organic PCMs are usually very low, it is still difficult to obtain significant enhancement in thermal conductivities by introducing high thermal conductive

[a]*CAS Key Laboratory of Cryogenics, Technical Institute of Physics and Chemistry, Chinese Academy of Sciences, Beijing 100190, China. E-mail: zsdeng@mail.ipc.ac.cn*
[b]*School of Future Technology, University of Chinese Academy of Sciences, Beijing 100049, China*

materials. At the same time, the introduction of a large amounts of enhancers that does not undergo phase change will cause inevitable latent heat loss and weight increase.

A main challenge of applying liquid metal to thermal management system as PCM is that the density is too high to be suitable for weight-sensitive applications.[14] In order to achieve lightweight, hollow glass microspheres have been incorporated into liquid metal to prepare a composite that can even float on water.[15] However, hollow glass microspheres are not suitable for use in PCC for the natural negative effects on thermal conductivity. The supercooling problem of gallium-based liquid metal is another challenge that affects the application in PCMs. Zhang *et al.* systematically studied the effects of thermal history and nucleating agent particle on the undercooling of gallium, and concluded that 0.5 wt% TeO_2 works best among various additives.[16] Considering the problem of corrosion between metal PCMs and metal container, Huang *et al.* and Liu *et al.* mixed low melting point alloys with melting points at about 70 and 140 °C respectively with EG, and utilized the porous microstructure to constraint the liquid metal, meanwhile, by adjusting the pressure during the molding, the apparent density of the PCC can also get controlled.[17,18] Similar to the reports on the organic PCMs, the graphite network was also used to improve the thermal conductivity of PCC, which was discussed earlier in the study about compressed expanded natural graphite by Zhong *et al.*[19] In addition to EG, graphite foam has also been shown to substantially increase the thermal conductivity of Wood's alloy.[20] Zhao *et al.* impregnated low melting point alloys into poco foam (carbon foam), and the performance of PCMs was effectively improved.[21] Also using copper foams as high thermal conductivity matrix, to prepare a thermal buffer, Yang *et al.* infiltrated field's alloys into copper foams to improve the thermal conductivity of PCC.[22]

Despite the efforts of previous researchers, obtaining perfect PCMs that is excellent in all aspects is still a formidable challenge, so a more realistic strategy is to create more PCM candidates to meet the different requirements. This means that it is necessary to adjust the thermophysical parameters of PCMs (or PCC) in a wide range. It is worth noting that organic PCMs and metal PCMs are highly complementary in properties such as latent heat, density, thermal conductivity, and cost, so an organic/metal PCC that compromise the properties of the two types of material will definitely bring about more new options. However, to the best of our knowledge, there is no report on such organic/metal PCC, and most researchers focus on making the two types of material play their respective roles with various additives. For example, Raj *et al.* added 5 wt% nano-encapsulated liquid eutectic Ga–In alloy to organo-metallic Mn based layered perovskite solid–solid PCM (SS-PCM), although both thermal conductivity and phase change enthalpy were improved, the thermal conductivity is still at a low level.[23] Salyan *et al.* mixed 0.1 wt% and 0.5 wt% gallium with D-Mannitol by ball milling, and gallium played the role of thermal conductivity enhancer and nucleating agent in the composite.[24] In order to reduce the weight and cost of the liquid metal PCM heat sink, Huang *et al.* proposed and numerically analyzed a dual PCMs heat sink, which can even achieve the effect close to that of a pure liquid metal heat sink by adjusting the ratio of liquid metal and paraffin arranged alternately.[25] Yu *et al.* designed a macro phase change capsule with eutectic Bi–In–Sn alloy/EG/Ecoflex composite as the elastic shell and octadecane as the core, the alloy improved the thermal conductivity of the shell and also contributed 20% of the latent heat density.[26] The above works either involve only a small amount of liquid metal or still separate the metal and the organic rather than effectively mixing, failing to achieve the desired organic/metal PCC.

Due to the huge difference in properties between organic and metal, it is very difficult to directly mix them and form a stable composite. Here, considering that EG with low density and high thermal conductivity has been successfully used to encapsulate a variety of PCMs, we used EG as a carrier to encapsulate octadecane and gallium uniformly, forming a class of organic/metal PCC with adjustable properties. Combined with the distribution of octadecane and gallium in the PCC and the DSC test results of the samples, the potential dispersant effect of octadecane on gallium and the phase change behavior were discussed. According to the DSC test results, the inhibitory effect of EG on the undercooling of gallium was revealed. Due to the complementary properties of octadecane and gallium, a variety of PCCs with vastly different properties can be obtained by adjusting the formulation. The structural stability of octadecane/gallium PCC was investigated by examining the appearance and weight changes of the PCC before and after phase change, respectively. The corrosion characteristics of the PCC was evaluated through the appearance change of the aluminum foil substrate contacted with the sample. The chemical stability was tested by comparing FT-IR spectrum. Through the DSC curves before and after 100 thermal cycles, the phase change performance stability was evaluated. The passive thermal management performance of octadecane/gallium PCC was also compared respectively with octadecane and gallium, proving its application value in related fields.

2. Material and methods

2.1. Preparation of PCC

As shown in Fig. 1, first, expandable graphite (Shanghai Aladdin Biochemical Technology Co., Ltd., China) was placed in a drying oven at 100 °C for 6 hours to remove moisture. Then put expandable graphite in the beaker, and place it in a 700 W microwave oven (Midea Inc., China) for 1 minute continuous heating to prepare EG.

Octadecane (99%, Shanghai Macklin Biochemical Co., Ltd., China) and gallium (99.99%, Hangzhou Keneng New Material Co., Ltd., China) were melted in a water bath at 40 °C and added into the beaker contained with EG. Then the mixture was continuously stirred for 30 minutes by a mechanical mixer at 400 rpm in a 60 °C water bath to achieve uniform PCC. In this study, the mass fraction of EG was controlled at 5%, and 7 kinds of PCCs with different ratios of octadecane and gallium were prepared and named as PCC 1–7. The mass ratios of octadecane and gallium are listed in Table 1.

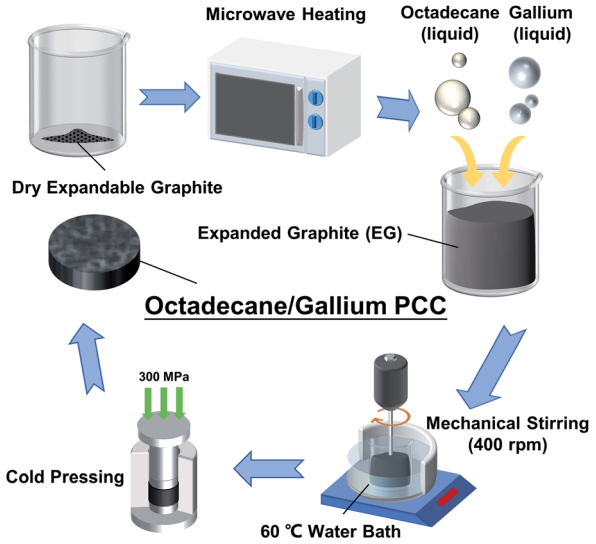

Fig. 1 Schematic diagram of the preparation process of octadecane/gallium PCC.

Table 1 Composition of samples

Sample number	Mass ratio of octadecane to gallium	Content of EG (wt%)
PCC 1	Octadecane only	5
PCC 2	5 : 1	5
PCC 3	3 : 1	5
PCC 4	1 : 1	5
PCC 5	1 : 3	5
PCC 6	1 : 5	5
PCC 7	Gallium only	5

After cooling to ambient temperature, the above-mentioned samples were transferred to a mold, then cold-compressed at 300 MPa for 1 minute to form a block-shaped PCC for subsequent testing and characterization. Before cold pressing, the mold and the PCC in it need to be put into the refrigerator at −80 °C for 5 minutes to avoid leakage of octadecane and gallium during the compression process.

2.2. Property characterization

A scanning electron microscope (QUANTA FEG 250, FEI, USA) was used to observe the microstructure of EG and PCCs. The melting point, latent heat, subcooling degree, and specific heat capacity of the PCCs were measured with differential scanning calorimetry (DSC, equipment model: NETZSCH DSC 200F3Maia). During DSC test, the temperature range was set from −40 to 60 °C and the same rate of 10 °C min^{-1} was applied for temperature control during both cooling and heating procedures. Isothermal stages with 5 minutes were set after cooling and heating, respectively. The densities of these samples were measured with the assistance of the drainage method density measurement component of precision balance (XSE105, METTLER TOLEDO). Combined with the density measured above, the thermal conductivity of bulk samples at 20 °C was measured and calculated by the laser flash analyzer (LFA467, NETZSCH).

To test the structural stability of the PCCs during the phase change process, the samples were placed in a drying oven at 40 °C for 30 minutes and cooled down to room temperature. This process was repeated 3 times. In order to see if there is a risk of corrosion to other structural metals caused by gallium leakage, each sample was placed on a piece of aluminum foil that had been sanded to remove the oxide, while a gallium droplet weighing 300 mg (almost equal to the gallium content in PCC 4) was placed on the surface of aluminum foil, served as a control group for corrosion phenomena.

The chemical stability was evaluated by comparing the results of the Fourier transform infrared spectroscopy (Excalibur 3100, varian, USA) before and after the above process. By comparing DSC results before and after 100 thermal cycles consistent with the DSC test described above, the thermal stability of the material after multiple thermal cycles was examined.

2.3. Thermal management performance test

The test bench for thermal management performance includes a heat source, a PCM container made of stainless steel, a laptop and an Agilent 34970 Data Acquisition Unit. The volume of the PCM in container was controlled at 10 mL (liquid volume for octadecane and gallium), and the temperature was measured with a type T thermocouple placed at the center of the bottom surface of the container. The heat source was wrapped in insulation foam except for the contact surface with the container. The thermal management performance of PCC 4 was evaluated according to the temperature response curves under different heat fluxes, and compared respectively with the performances of octadecane and gallium. For the periodic thermal shock test, in one cycle, the heat flux was set as 7500 W m^{-2}, and after continuous heating for 3 minutes, the device was cooled down with fan assistance for 12 minutes. The above process was repeated 10 times.

3. Result and discussion

3.1. Morphological characterization

The PCCs obtained after cold pressing are in the shape of solid cylindrical blocks. After cutting the PCC 1–7 vertically, the micro morphology on the cross section is observed with SEM to analyze the distribution of octadecane and gallium in the composites. The microscopic images of EG and PCCs are shown in Fig. 2. As shown in Fig. 2(a), there are scalelike structures and micron-sized pores on the surface of EG. As exhibited in Table 1, PCC 1 does not contain gallium, so the material filled between the scalelike structures in Fig. 2(b) is octadecane. Obviously, octadecane can fully penetrate into EG. As the addition of gallium increases, the presence of gallium particles can be clearly observed in the SEM images (Fig. 2(c)–(h)). It could be seen that, unlike octadecane, gallium cannot entirely penetrate into the crevices on the surface of EG and can just adhere to the larger cavities. Considering that the permeation and adsorption

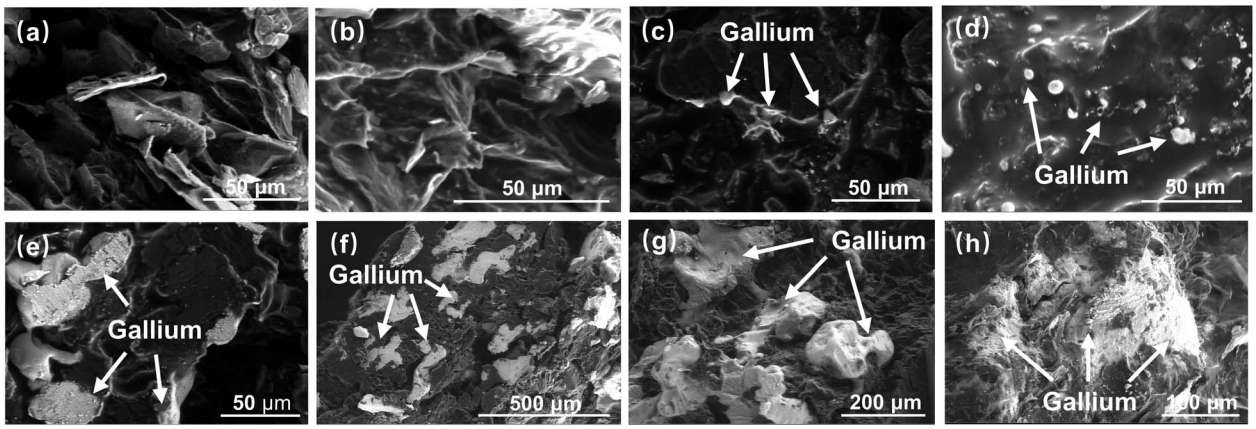

Fig. 2 SEM images of EG and PCCs. (a) EG. (b) PCC 1. (c) PCC 2. (d) PCC 3. (e) PCC 4. (f) PCC 5. (g) PCC 6. (h) PCC 7.

are affected by capillary force and surface tension, it is more difficult for gallium with larger surface tension to directly enter into smaller pores, resulting in this distribution difference. The size and number of gallium particles embedded in the middle of the composites increase with the increase of the mass fraction of gallium. For example, in Fig. 2(c), only sporadic micron-sized gallium particles can be seen, while in Fig. 2(g), it can be clearly seen that gallium particles with diameter of more than 100 μm are embedded in the composite. At the same time as the gallium content rises, the gallium dispersibility gets worse, so that in the case of the complete absence of octadecane, it can be seen in Fig. 2(h) that the undispersed gallium is squeezed into the EG matrix. In addition to the increased difficulty of dispersion due to the increased gallium content, this change in metal dispersibility also suggests that octadecane likely played a role as dispersant during the preparation. The above results of the internal micro-morphology of PCCs indicate that the effective mixing of octadecane and gallium mediated by EG can be achieved by mechanical stirring, and then uniform organic/metal PCC with graphite framework can be formed after cold pressing.

3.2. Thermophysical properties of PCC

For thermal management or energy storage, the phase change properties of PCMs are crucial. By analyzing the DSC curves, the melting point, latent heat of melting, and subcooling degree of each sample can be obtained.

In addition to the curves of each PCC introduced in Table 1, Fig. 3(a) also shows the DSC curves of octadecane and gallium as raw materials to illustrate the change in the phase change behavior after the materials are composited together. The phase change properties of these materials are shown in Table 2.

It can be deduced from Fig. 3(a) that the supercooling degree of gallium is 58.4 °C under the test condition described above, while octadecane has almost no supercooling. Furthermore, it is worth noting that, in Fig. 3(b), except for the presence of severe undercooling in a small fraction, the main solidification peak of PCC 7 has moved to the position corresponding to the freezing point of 22.9 °C, and the degree of supercooling is reduced by 86.82% compared with that for pure gallium. The research of Zhang *et al.*, showed that, the nucleating agent of gallium should have a lattice constant close to that of gallium,[16] but it is known that graphite does not meet this condition, so the decrease of supercooling degree is unlikely to be owing to the nucleation effect of EG. The possible cause of this phenomenon is that some micro gallium droplets or particles are adsorbed or squeezed into the narrow cavities and cracks of EG under the pressure during the mechanical stirring and cold pressing to form nucleation embryos. According to Turnbull's theory, these embryos can be retained even the temperature exceeds the melting point, and when the radius at the cavity opening equals or exceeds the critical radius for nucleation, the solidification of the supercooled liquid can be triggered.[27] In fact, seeding is already a common nucleation-triggering strategy, and in this study, EG with complex micro-porous structures may well play a similar role while supporting and encapsulating metal PCMs.[28]

The suppression effect of EG on subcooling is also reflected in the DSC results of PCC 2–6, which are mixtures of octadecane and gallium mediated by EG. As shown in Fig. 3(c), it is worth noting that with the increase of octadecane content, the decrease of supercooling degree is more obvious, which may be related to the dispersing effect of octadecane that facilitates the generation and preservation of small gallium particles as nucleation embryos.

In addition to the above seeding mechanism, the latent heat of octadecane per unit mass is nearly 3 times that of gallium, which is reflected in the DSC curves that the peak area of the former is also nearly 3 times that of the latter. Although the melting point of octadecane is slightly lower than that of gallium, the phase change peak of gallium is completely covered by octadecane in Fig. 3(c), resulting in that the DSC curves of PCC 1–4 are closer to octadecane. Only when the mass of gallium in the composite reaches more than 3 times that of octadecane, the phase change characteristics of gallium (*e.g.*, supercooling) can be displayed more clearly, making the supercooling inhibitory effect of PCC 5–6 appear to be reduced. In addition to the degree of subcooling, a similar effect can be

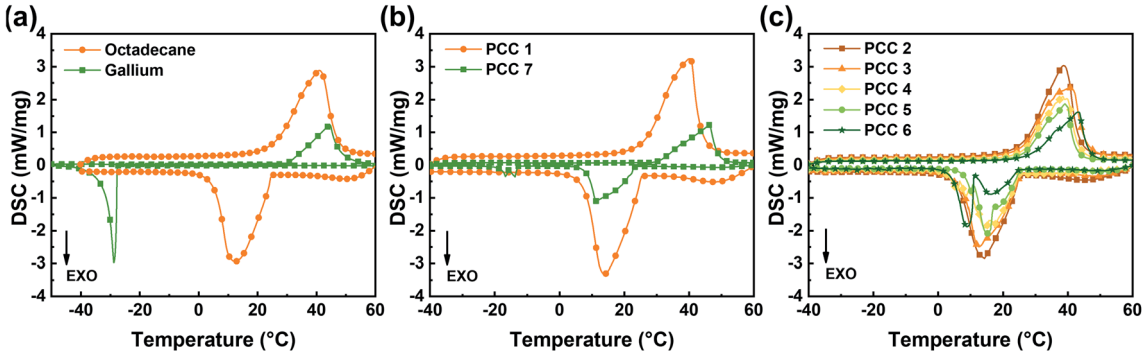

Fig. 3 DSC curves of octadecane, gallium and PCC. (a) octadecane and gallium. (b) PCC 1 and PCC 7. (c) PCC 2–6.

observed on the melting point of composite. Until the mass of gallium reaches 3 times that of octadecane, the measured melting point of the composite is close to octadecane.

From the experimental data shown in Table 2, the melting latent heat of the PCC is affected by the mass ratio of octadecane to gallium. As the gallium content increases, the latent heat of the CPCM gradually decreases. The theoretical melting latent heat ΔH_t of the PCC can be calculated by eqn (1):

$$\Delta H_t = \Delta H_{oct} w_{oct} + \Delta H_{ga} w_{ga} \quad (1)$$

where ΔH_{oct} and ΔH_{ga} represent the melting latent heat of octadecane and gallium; w_{oct} and w_{ga} represent the mass fraction of two raw PCMs of the PCC, respectively. As shown in Table 2, all the relative errors between the experimental results of the melting latent heat and the theoretical values are less than 6%. Due to the random sampling during the test, this result indicates that after stirring and cold pressing, the distribution of octadecane and gallium in the sample is uniform.

Considering that in actual use, the space left for PCMs is often limited, so the latent heat per unit volume of PCC is sometimes more meaningful than the latent heat per unit mass. After the density of the sample is measured by the drainage method, the latent heat storage density (*i.e.*, the latent heat per unit volume) can be calculated using eqn (2):

$$\Delta H_v = \rho \Delta H_m \quad (2)$$

The latent heat storage density of the samples is shown in Fig. 4(a), and its changing trend with the increase of gallium content is opposite to the latent heat of melting, which is due to the fact that the energy storage density of gallium is nearly 2 times higher than that of octadecane. Besides, as the gallium content increases, shown in Fig. 4(b), the density and thermal conductivity of the sample increases simultaneously. The reason for this synchronization is that the density and thermal conductivity of gallium are much larger, which has a decisive influence on the final density and thermal conductivity of the composites. Since gallium is dispersed and embedded in the EG impregnated with octadecane, it is relatively difficult to form a thermally conductive path, and then the thermal conductivity of the composite has a slower response to the gallium content as compared with density. Although EG could improve thermal conductivity and adjust density in previous studies on organic PCMs, considering the consistent mass fraction of EG in each PCC sample, the thermal conductivity and density of PCC 1–7 in this study are dominated by the ratio of octadecane to gallium. In other words, after EG-mediated mixing, octadecane is a lightweight additive with considerable latent heat for gallium, while gallium is an enhancer of thermal conductivity and energy storage density for octadecane.

In order to more intuitively show the distribution range and variation of the above thermophysical properties, the density,

Table 2 Phase change properties of raw materials and samples[a]

PCM	T_m (°C)	Subcooling degree (°C)	ΔH_m (J g^{-1})	ΔH_t (J g^{-1})	Relative error (%)
Octadecane	25.4	0.8	215.00	—	—
Gallium	30.7	58.4	78.01	—	—
PCC 1	26	0.8	211.00	204.25	3.30
PCC 2	25.8	0.9	187.30	182.54	2.61
PCC 3	25.8	0.6	176.70	171.71	2.91
PCC 4	25.8	0.8	136.40	139.18	2.42
PCC 5	25.9	0.7 (8.7) (15.1)	106.80	106.64	0.15
PCC 6	28.9	3.9 (17.5)	99.83	95.82	4.18
PCC 7	30.6	7.7 (50)	70.19	74.11	5.29

[a] When the DSC curve of a PCC has multiple solidification points, the higher degree of subcooling is recorded in parentheses.

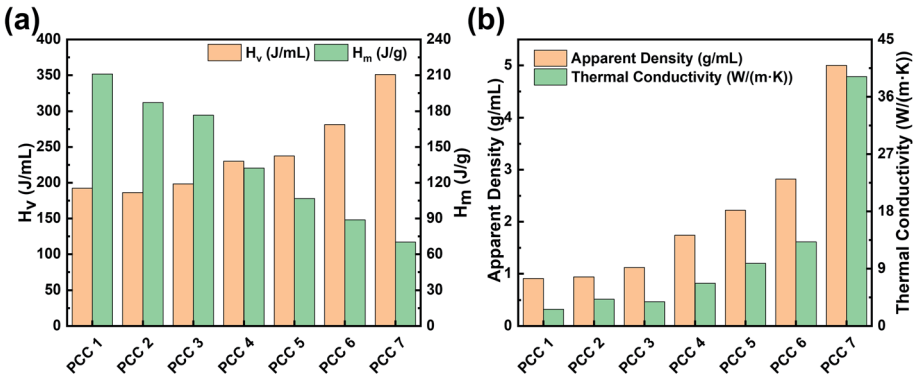

Fig. 4 Latent heat storage density, apparent density and thermal conductivity of PCC. (a) Comparison of latent heat of melting and storage density. (b) Apparent density and thermal conductivity.

latent heat and thermal conductivity of the PCC 1–7 are integrated in Fig. 5. The area of the colored part on the x–y plane corresponds to the energy storage density of the sample. PCC 1 and PCC 7 are two extreme points. In theory, each PCC on the curve between the two extreme points can be prepared by the method proposed in this study to obtain the corresponding properties.

Table 3 gives a comparison of the thermophysical properties of octadecane/gallium PCC with those of PCCs in the recent literature. To enhance the comparability of data, the melting points of the selected PCCs are all close to those of octadecane/gallium PCC (about 20–45 °C). Density was not considered in this comparison since it was not a concern in some studies. It is easy to see that the existing studies are unlikely to achieve the same large-scale performance tuning as this work by adjusting the material ratios. At the same time, the thermophysical properties of octadecane/gallium PCC proposed in this work are also competitive within this melting point range.

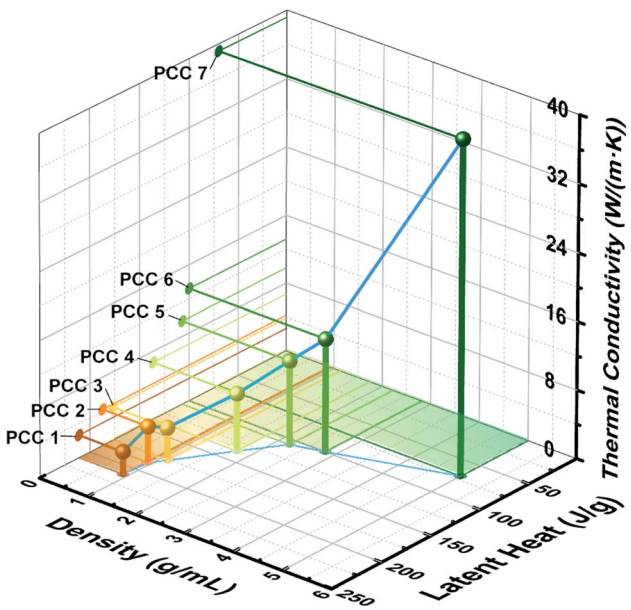

Fig. 5 The distribution of PCC thermophysical properties.

Since the specific heat capacity measures the ability of the material to store sensible heat before and after phase change, it is also an important thermophysical property of PCM in addition to the latent heat. Fig. 6 shows the specific heat-temperature curves of the PCC before and after phase change. Different from the change pattern of density and thermal conductivity, the specific heat of the sample with more octadecane is significantly larger before and after phase change due to the greater specific heat of octadecane compared to gallium.

Due to the existence of latent heat, phase change can roughly be regarded as a heat exchange process with high equivalent specific heat. Therefore, the specific heat curves rise and fall significantly before (Fig. 6(a)) and after (Fig. 6(b)) phase change. Since octadecane is an amorphous PCM, it can be seen in Fig. 6(a) that the curve of PCC 1 has already started to rise rapidly before the temperature reaches the melting point (26 °C), which means that a part of the octadecane begins to absorb latent heat prematurely. This phenomenon is a potential disadvantage for thermal management applications. In contrast, the curve of PCC 7 without octadecane is almost completely horizontal before the melting point. In organic/metallic PCCs, the situation is improved with increasing gallium content, showing that although octadecane has greater effect on the melting point, the presence of gallium makes the phase change region of the PCC more concentrated.

3.3. Structural and chemical stability analysis

It is very important to its normal function for PCC to maintain its structure, composition, and properties during phase change. Since the PCMs are impregnated inside the EG, the PCCs obtained after cold pressing are apparently a solid–solid PCMs, which is beneficial to suppress the volume change in phase change and also reflects the structural stability. Fig. 7(a) shows the changes in appearance of PCC 1–7 before and after structural stability test. Structurally, each sample maintained its initial state. More leaked octadecane was observed around PCC 1 and the edges of the structure became blurred. More metal distribution was observed on the surface of each organic/metallic PCC than before the test, but no spherical droplets, which are characteristic of liquid metal leakage,[17] were

Table 3 Comparison of thermal properties of octadecane/gallium PCC with those of PCCs in the literature

PCM	Carrier	ΔH_m (J g^{-1})	Thermal conductivity (W (m^{-1} K^{-1}))	Ref.
Eutectic hydrated salt	Porous diatomite & PUA	99.8–109.7	0.32–0.41	29
Paraffin	Scaffold loaded with SiCNFs	180.5	1.29	30
Eutectic hydrated salt	Macro-porous melamine sponge & PU	186.6	0.2287	31
Fatty acid	Diatomite & EG	75.84–87.33	0.219–0.467	32
Paraffin	CNTs/EP	95.98–103.85	0.107–0.516	33
Paraffin	CNTs/EP	157.43–161.18	0.15–0.32	34
Gallium & octadecane	EG	70.19–211	2.639–39.158	This work

observed. However, this phenomenon is not as pronounced on the surface of PCC 7 containing only gallium and the highest content of gallium compared with that of organic/metallic PCC, indicating that octadecane also plays an important role behind this phenomenon. In the melting process, octadecane and gallium have three main differences: (a) octadecane has a slightly lower melting point, so it melts before gallium; (b) when octadecane melts, its volume expands while gallium contracts abnormally; (c) liquid octadecane has lower surface tension, more likely to flow out of EG. According to the study of Lopez *et al.*, in the composite composed of graphite and PCM, the volume expansion of the PCM during the melting process will cause the internal pressure increase,[35] and Huang *et al.* also pointed out that if the pressure increase is not released, the liquid Wood's Alloy will be squeezed out.[17] Different from most PCMs, gallium shrinks during the melting process, so for PCC 7, the overpressure problem summarized in previous research is not a concern. When octadecane is present, the melted octadecane may flow out to expose some of the metal that was previously covered. In addition, as mentioned in the previous section, octadecane can easily penetrate into the microstructure of EG, reducing the porosity, while gallium can only be adsorbed on larger pores and cracks. This means that when the octadecane overflows due to expansion, gallium is likely to block on the channel, thereby being pushed towards the surface of the composite. Since octadecane will choose the route with lower resistance, the thrust and extrusion on gallium are limited, leaving most of the gallium still embedded in the composite rather than being extruded into spherical particles.

To determine if serious gallium leakage occurred, the samples were placed on the aluminum foil polished in advance. Gallium droplet was used as control. As shown in Fig. 7, the gallium droplets caused severe corrosion to the aluminum foil. Fig. 7(b) shows the contact surface between the sample and the aluminum foil before and after the test. The results show that the PCC almost caused no change to the aluminum foil, indicating that the corrosion risk caused by gallium leakage has been effectively suppressed. The mass loss rates of PCC 1–7 during the test are 10.79%, 8.37%, 4.86%, 1.42%, 0.62%, 0.07%, and 0.02%, respectively. It can be concluded that the loss rate decreases with the decrease of octadecane content. For PCC 7 containing only gallium, the mass loss is negligible, indicating that the leakage for the PCC is mainly octadecane rather than gallium. As for how to further reduce the leakage of octadecane, according to experience, it can be adjusted by changing the mass fraction of EG and the pressure during the cold pressing, which is worthy of further study.

By comparing the FT-IR spectrum of Fig. 8(a) and (b), it can be seen that there is no significant change in the positions of absorption bands after the test, which indicates that these PCCs

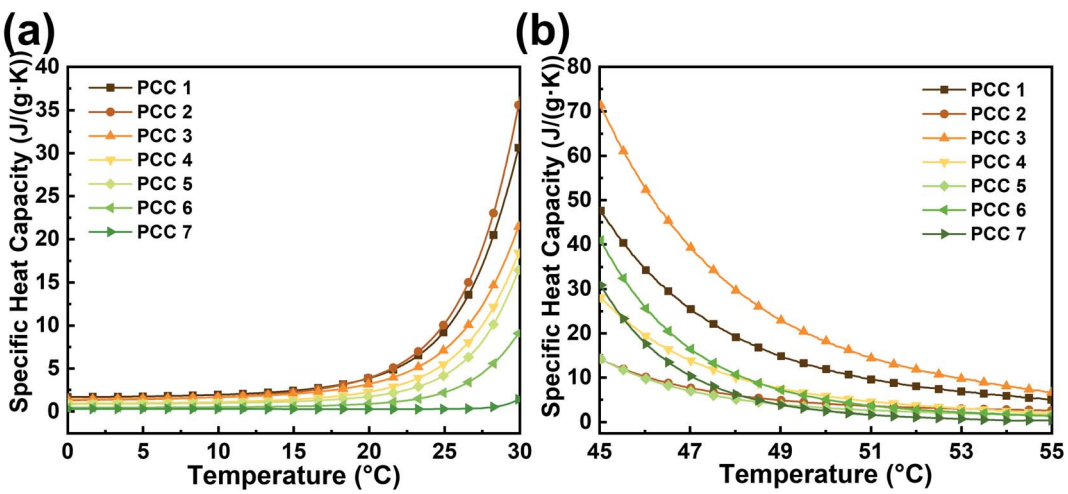

Fig. 6 Specific heat capacity – temperature curves of samples (a) before and (b) after the phase change.

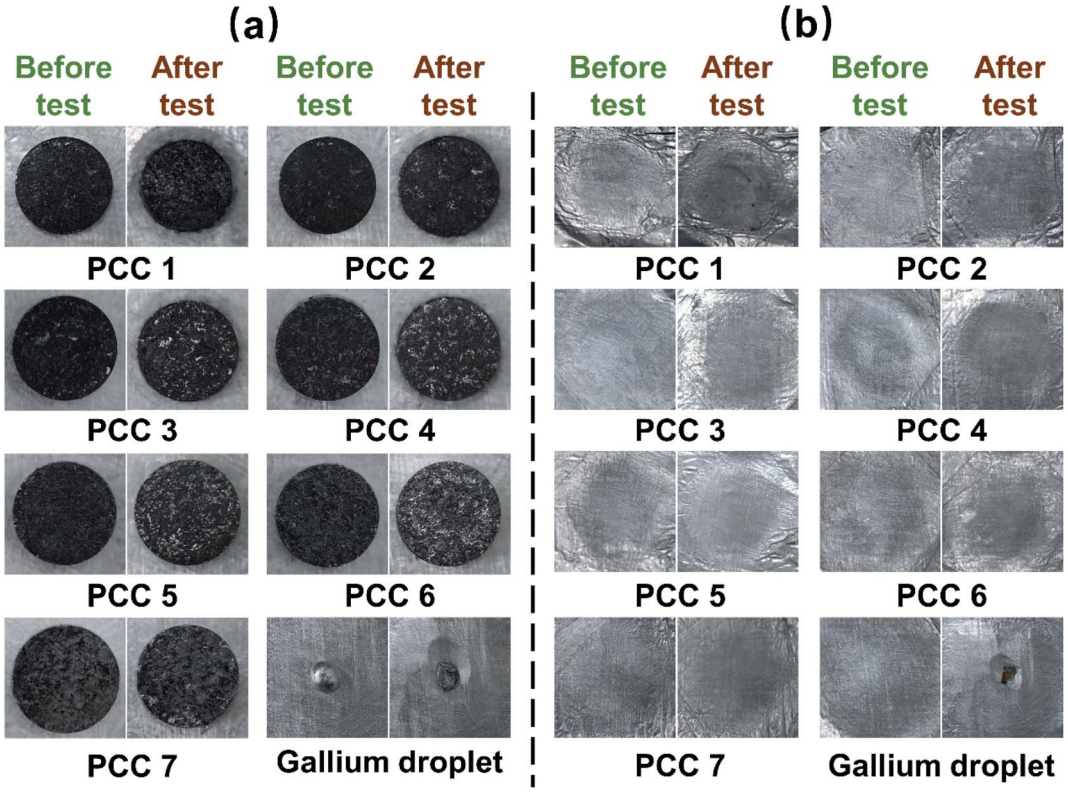

Fig. 7 Structural stability test results. (a) Appearance of the samples and the control group before and after the test; (b) the contact surface of the sample and the control group with the polished aluminum foil before and after the test.

possess a good chemical stability during the phase change cycles. Except for PCC 7, which has almost no response peak, the positions of absorption bands of the other samples are consistent with PCC 1, which indicates that gallium and octadecane are independent of each other in the system without chemical reaction.

As shown in Fig. 9, the DSC curves of PCC 4 before and after 100 thermal cycles almost overlap, which means that the main thermophysical parameters such as melting point, freezing point, subcooling, latent heat remain stable during repeated melting and freezing processes, indicating its excellent performance in thermal stability.

3.4. Thermal management performance

Considering that the thermophysical parameters of PCC 4 are all at the intermediate level, it was selected to investigate the thermal performance of the composite. Using the experimental device shown in Fig. 10(a), the passive thermal management performance was evaluated by testing the ability of the octadecane/gallium PCC to control the interface temperature within 30 minutes under the shock of 2500–10 000 W m^{-2} heat flux (Fig. 10(b)). With the increase of heat flux, the final interface temperature increases gradually. For 2500 and 5000 W m^{-2} heat flux, PCC 4 has a relatively good

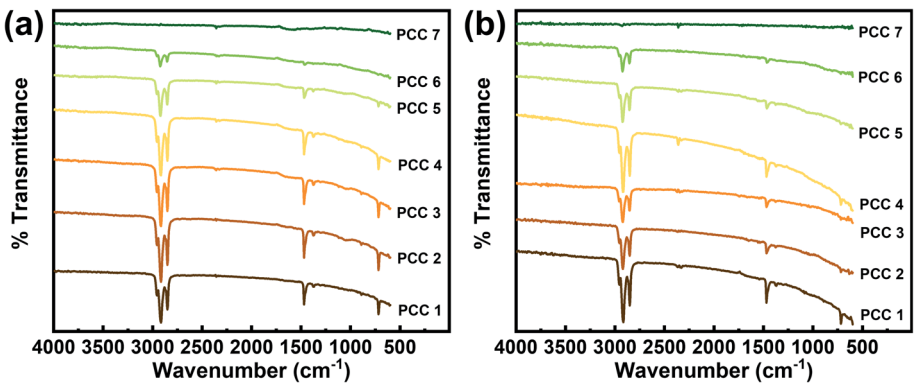

Fig. 8 Fourier transform infrared spectroscopy of PCCs (a) before and (b) after phase change.

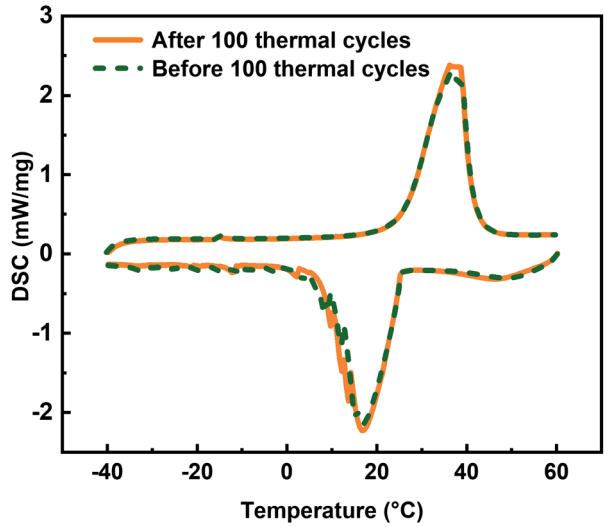

Fig. 9 DSC curves of PCC 4 before and after 100 thermal cycles.

thermal management performance and can maintain the interface temperature within 30 minutes lower than 45 °C. Until the heat flux reaches 10 000 W m^{-2}, the PCC still has good performance in temperature control. As mentioned above, organic PCMs and metal PCMs have obvious complementarity, so the PCC proposed in this study is a good balance between the properties of octadecane and gallium. To further demonstrate this, octadecane, PCC 4 and gallium were tested against the same heat flux. As shown in Fig. 10(c), the temperature response curve of PCC 4 is indeed located in the middle position of octadecane and gallium. Considering that in the thermal management applications with PCMs, the chips or devices often work intermittently, the periodic thermal shock test is performed with heat flux of 7500 W m^{-2}. Each cycle consists of 3 minutes of heating and 12 minutes of forced air cooling. As shown in Fig. 10(d), the highest temperature gradually increased for the first four cycles, and then stabilized at 40.723 to 41.348 °C since the fifth cycle. Compared with the temperature increase for the case without PCM, PCC 4 shows excellent performance in temperature control. Combined with the material properties and the above test results, it indicates that PCC 4 has the potential to be used in phase change thermal control for wearable electronic devices, interactive device or related applications, where thermal comfort for human body is a major concern.

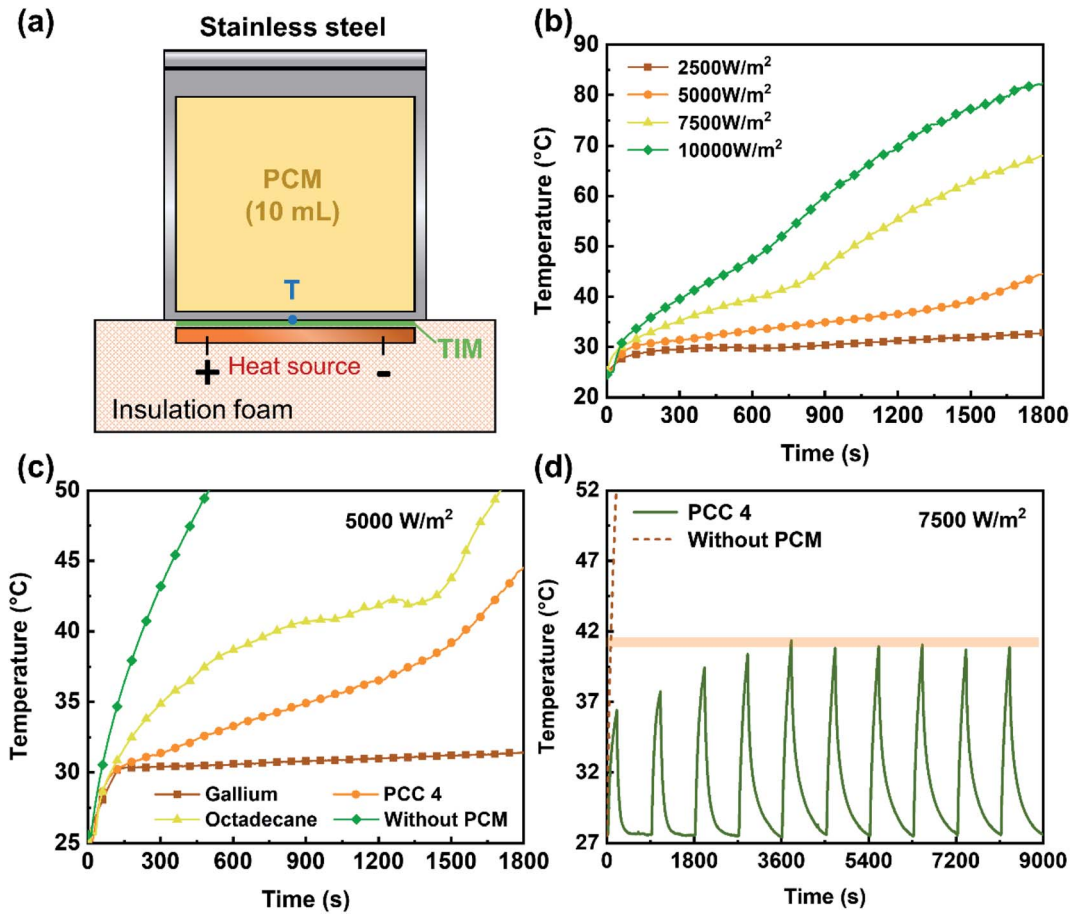

Fig. 10 Thermal management performance test setup and results. (a) Schematic diagram of the experimental setup; (b) temperature response curves at different heat fluxes; (c) temperature response curves of octadecane, gallium and PCC 4 at heat flux of 5000 W m^2; (d) temperature response under periodic thermal shock test.

4. Conclusion

In this study, using EG as a carrier of octadecane and gallium, a novel organic/metallic PCC was successfully prepared by stirring and cold pressing. The SEM images of the samples show that octadecane can be fully impregnated into the microstructure of EG, and the gallium is packed in larger pores and crevices with a relatively uniform distribution. The DSC test results show that the introduction of EG can effectively suppress the undercooling of gallium, which may be related to the preservation of gallium embryos in the microcavity of EG. Since the thermophysical properties of octadecane and gallium are highly complementary, by changing the formulation, the properties of the PCC proposed in this study can be adjusted in a wide range. For the tested samples of octadecane/gallium PCC, the density can vary from 0.912 to 4.998 g mL^{-1}, the corresponding latent heat can vary from 211 to 70.19 J g^{-1}, and the corresponding thermal conductivity can vary from 2.639 to 39.158 W (m^{-1} K^{-1}). In general, the latent heat is the result of a proportional balance between octadecane and gallium. Octadecane dominates latent heat of melting and specific heat capacity while reducing the weight. Gallium dominates energy storage density and thermal conductivity while making the phase change range of PCC more concentrated. The PCC has good structural stability, and can effectively suppress the leakage of gallium during the phase change process, thereby reducing the risk of corrosion. The results also indicate its excellent performance in chemical and thermal stabilities. Thermal management testing shows that the PCC has excellent performance in temperature control, and the potential to be used in phase change thermal control for wearable electronic devices, interactive device or related applications. The octadecane/gallium PCC proposed in this study creates more candidate PCMs for related fields, and provides new idea and guidance for subsequent researchers to prepare PCCs with desired properties. Since this study mainly focused on the property balance between octadecane and gallium, the mass fraction of EG and preparation process are fixed, and their influence on the final performance deserves more research in the future. In addition, the influence of other additives such as nanoparticles on the composite system is also worthy of further discussion in the future.

Author contributions

Yuchen Yao, and Zhongshan Deng conceived the idea. Yuchen Yao and Yuntao Cui carried out most of the experiments. Yuchen Yao and Zhongshan Deng composed the first version of the manuscript. All authors participated in interpretation of the results and helped revising the manuscript.

Conflicts of interest

There are no conflicts to declare.

Acknowledgements

This work is supported by the Genetic Engineering of Rare Precious Metal Materials in Yunnan Province, and No. CRYOQN202109, the Youth Science and Technology Innovation Project of Key Lab of Cryogenics, Chinese Academy of Sciences.

References

1 H. Ge, H. Li, S. Mei and J. Liu, Low Melting Point Liquid Metal as a New Class of Phase Change Material: An Emerging Frontier in Energy Area, *Renewable Sustainable Energy Rev.*, 2013, **21**, 331–346.
2 S. Zhu, M. T. Nguyen and T. Yonezawa, Micro- and Nano-Encapsulated Metal and Alloy-Based Phase-Change Materials for Thermal Energy Storage, *Nanoscale Adv.*, 2021, **3**(16), 4626–4645.
3 S. C. Costa and M. Kenisarin, A Review of Metallic Materials for Latent Heat Thermal Energy Storage: Thermophysical Properties, Applications, and Challenges, *Renewable Sustainable Energy Rev.*, 2022, **154**, 111812.
4 H. Ge and J. Liu, Phase Change Effect of Low Melting Point Metal for an Automatic Cooling of Usb Flash Memory, *Front. Energy*, 2012, **6**(3), 207–209.
5 H. Ge and J. Liu, Keeping Smartphones Cool with Gallium Phase Change Material, *J. Heat Transfer*, 2013, **135**(5), 054503.
6 S. Xiang, D. Liu, C. Jiang, W. Zhou, D. Ling, W. Zheng, X. Sun, X. Li, Y. Mao and C. Shan, Liquid-Metal-Based Dynamic Thermoregulating and Self-Powered Electronic Skin, *Adv. Funct. Mater.*, 2021, **31**(26), 2100940.
7 H. Peng, W. Guo, M. Li and S. Feng, Melting Behavior and Heat Transfer Performance of Gallium for Spacecraft Thermal Energy Storage Application, *Energy*, 2021, **228**, 120575.
8 S. K. Sahoo, M. K. Das and P. Rath, Application of Tce-Pcm Based Heat Sinks for Cooling of Electronic Components: A Review, *Renewable Sustainable Energy Rev.*, 2016, **59**, 550–582.
9 C. Reuben Raj, S. Suresh, S. Vasudevan, M. Chandrasekar, V. Kumar Singh and R. R. Bhavsar, Thermal Performance of Nano-Enriched Form-Stable Pcm Implanted in a Pin Finned Wall-Less Heat Sink for Thermal Management Application, *Energy Convers. Manage.*, 2020, **226**, 113466.
10 Z. Zhang and X. Fang, Study on Paraffin/Expanded Graphite Composite Phase Change Thermal Energy Storage Material, *Energy Convers. Manage.*, 2006, **47**(3), 303–310.
11 S. Wang, P. Qin, X. Fang, Z. Zhang, S. Wang and X. Liu, A Novel Sebacic Acid/Expanded Graphite Composite Phase Change Material for Solar Thermal Medium-Temperature Applications, *Sol. Energy*, 2014, **99**, 283–290.
12 S. Wu, T. X. Li, T. Yan, Y. J. Dai and R. Z. Wang, High Performance Form-Stable Expanded Graphite/Stearic Acid Composite Phase Change Material for Modular Thermal Energy Storage, *Int. J. Heat Mass Transfer*, 2016, **102**, 733–744.
13 J. A. Duan, Novel Heat Sink for Cooling Concentrator Photovoltaic System Using Pcm-Porous System, *Appl. Therm. Eng.*, 2021, **186**, 116522.
14 X.-H. Yang, S.-C. Tan and J. Liu, Thermal Management of Li-Ion Battery with Liquid Metal, *Energy Convers. Manage.*, 2016, **117**, 577–585.

15 B. Yuan, C. Zhao, X. Sun and J. Liu, Lightweight Liquid Metal Entity, *Adv. Funct. Mater.*, 2020, **30**(14), 1910709.
16 C. Zhang, L. Li, X. Yang, J. Shi, L. Gui and J. Liu, Study on the Nucleating Agents for Gallium to Reduce Its Supercooling, *Int. J. Heat Mass Transfer*, 2020, **148**, 119055.
17 Z. Huang, Z. Luo, X. Gao, X. Fang, Y. Fang and Z. Zhang, Preparation and Thermal Property Analysis of Wood's Alloy/Expanded Graphite Composite as Highly Conductive Form-Stable Phase Change Material for Electronic Thermal Management, *Appl. Therm. Eng.*, 2017, **122**, 322–329.
18 L. Liu, J. Chen, Y. Qu, T. Xu, H. Wu, X. Zhou and H. Zhang, Preparation and Thermal Properties of Low Melting Point Alloy/Expanded Graphite Composite Phase Change Materials Used in Solar Water Storage System, *Sol. Energy Mater. Sol. Cells*, 2019, **201**, 110112.
19 Y. Zhong, Q. Guo, L. Li, X. Wang, J. Song, K. Xiao and F. Huang, Heat Transfer Improvement of Wood's Alloy Using Compressed Expanded Natural Graphite for Thermal Energy Storage, *Sol. Energy Mater. Sol. Cells*, 2012, **100**, 263–267.
20 Y. Zhong, Q. Guo, S. Li, J. Shi and L. Liu, Thermal and Mechanical Properties of Graphite Foam/Wood's Alloy Composite for Thermal Energy Storage, *Carbon*, 2010, **48**(5), 1689–1692.
21 L. Zhao, Y. Xing, Z. Wang and X. Liu, The Passive Thermal Management System for Electronic Device Using Low-Melting-Point Alloy as Phase Change Material, *Appl. Therm. Eng.*, 2017, **125**, 317–327.
22 T. Yang, J. G. Kang, P. B. Weisensee, B. Kwon, P. V. Braun, N. Miljkovic and W. P. King, A Composite Phase Change Material Thermal Buffer Based on Porous Metal Foam and Low-Melting-Temperature Metal Alloy, *Appl. Phys. Lett.*, 2020, **116**(7), 071901.
23 C. R. Raj, S. Suresh, V. K. Singh, R. R. Bhavsar, M. V. C, S. Vasudevan and V. Archita, Experimental Investigation on Nanoalloy Enhanced Layered Perovskite Pcm Tamped in a Tapered Triangular Heat Sink for Satellite Avionics Thermal Management, *Int. J. Therm. Sci.*, 2021, **167**, 107007.
24 S. Salyan and S. Suresh, Liquid Metal Gallium Laden Organic Phase Change Material for Energy Storage: An Experimental Study, *Int. J. Hydrogen Energy*, 2018, **43**(4), 2469–2483.
25 P. Huang, G. Wei, L. Cui, C. Xu and X. Du, Numerical Investigation of a Dual-Pcm Heat Sink Using Low Melting Point Alloy and Paraffin, *Appl. Therm. Eng.*, 2021, **189**, 116702.
26 D.-H. Yu and Z.-Z. He, Shape-Remodeled Macrocapsule of Phase Change Materials for Thermal Energy Storage and Thermal Management, *Appl. Energy*, 2019, **247**, 503–516.
27 D. Turnbull, Kinetics of Heterogeneous Nucleation, *J. Chem. Phys.*, 1950, **18**(2), 198–203.
28 N. Beaupere, U. Soupremanien and L. Zalewski, Nucleation Triggering Methods in Supercooled Phase Change Materials (Pcm), a Review, *Thermochim. Acta*, 2018, **670**, 184–201.
29 N. Xie, J. Niu, Y. Zhong, X. Gao, Z. Zhang and Y. Fang, Development of polyurethane acrylate coated salt hydrate/diatomite form-stable phase change material with enhanced thermal stability for building energy storage, *Constr. Build. Mater.*, 2020, **259**, 119714.
30 X. Li, H. Wang, X. Yang, X. Zhang and B. Ma, Simple *in situ* synthesis of SiC nanofibers on graphite felt as a scaffold for improving performance of paraffin-based composite phase change materials, *RSC Adv.*, 2021, **12**, 878–887.
31 W. Chen, X. Liang, S. Wang, X. Gao, Z. Zhang and Y. Fang, Polyurethane macro-encapsulation for $CH_3COONa\ 3H_2O$-$Na_2S_2O_3\ 5H_2O$/melamine sponge to fabricate form-stable composite phase change material, *Chem. Eng. J.*, 2021, **410**, 128308.
32 R. Wen, X. Zhang, Z. Huang, M. Fang, Y. Liu, X. Wu, X. Min, W. Gao and S. Huang, Preparation and thermal properties of fatty acid/diatomite form-stable composite phase change material for thermal energy storage, *Sol. Energy Mater. Sol. Cells*, 2018, **178**, 273–279.
33 X. Zhang, R. Wen, Z. Huang, C. Tang, Y. Huang, Y. Liu, M. Fang, X. Wu, X. Min and Y. Xu, Enhancement of thermal conductivity by the introduction of carbon nanotubes as afiller in paraffin/expanded perlite form-stable phase-change materials, *Energy Build.*, 2017, **149**, 463–470.
34 A. Karaipekli, A. Biçer, A. Sarı and V. V. Tyagi, Thermal characteristics of expanded perlite/paraffin composite phase change material with enhanced thermal conductivity using carbon nanotubes, *Energy Convers. Manage.*, 2017, **134**, 373–381.
35 J. C. Lopez, G. Del Barrio and E. P. Jomaa, Confined melting in deformable porous media: afirst attempt to explain the graphite/salt composites behaviour, *Int. J. Heat Mass Transfer*, 2010, **53**, 1195–1207.